



**46º CONGRESO ESPAÑOL DE ACÚSTICA
ENCUENTRO IBÉRICO DE ACÚSTICA
SIMPOSIO EUROPEO SOBRE ACÚSTICA VIRTUAL Y
AMBISONICS**

**ON THE USE OF THE BEM TO STUDY THE NOISE EMITTED BY CIRCULATING
EVS OR HVS IN URBAN ENVIRONMENT**

PACS:43.50.Lj, 43.28.Js

Alba Sánchez-Milan¹, Jesus Carbajo², Luís Godinho³, Ramon Peral-Orts¹, Jaime Ramis-Soriano²

¹Departamento de Ingeniería Mecánica y Energía, Universidad Miguel-Hernandez, Elche, España

{albasanchezmilan@gmail.com, ramon.peral@umh.es}

²Departamento de Física, Universidad de Alicante, Carretera San Vicente del Raspeig, 03080, San Vicente del Raspeig, España

{jesus.carbajo@ua.es, jramis@ua.es}

³ISISE, Departamento de Engenharia Civil, Universidade de Coimbra, Rua Luís Reis Santos - Pólo II da Universidade, 3030-788 Coimbra, Portugal
{lgodinho@dec.uc.pt}

ABSTRACT

Existing literature addressed the problem of near-field sound emission from electrical and hybrid vehicles, which is of significant importance since it is the means of identifying the presence of these vehicles by visually impaired persons. Its simulation may be done using different methods, and it is crucial to include details such as the directivity of the sound source emitting warning sounds or Acoustic Vehicle Alerting Systems (AVAS). In this paper, the "ACA-BEM", complemented with adequate Green's functions, is used to conduct numerical studies regarding the effect of the AVAS in open street and in street with a lateral rigid wall configurations, and in the presence of other vehicles (acting as barriers).

RESUMO

Algumas publicações técnico-científicas abordam o problema da emissão sonora de campo próximo de veículos elétricos e híbridos. Esta emissão é de grande importância, uma vez que é o meio de identificar a presença desses veículos por pessoas com deficiência visual. A simulação do comportamento destes veículos pode ser feita usando métodos diferentes, e é crucial para incluir detalhes como a diretividade da fonte sonora que emite ruídos de alerta do veículo ou Acoustic Vehicle Alerting Systems (AVAS). Neste trabalho, o "ACA-BEM", complementado com funções de Green adequadas, é utilizado para conduzir estudos numéricos sobre o efeito do AVAS em configurações abertas e numa rua com uma parede rígida laterais, e na presença de outros veículos (actuando como barreira).

INTRODUCTION

It is known that, at low speed, Electric Vehicles (EVs) produce very little noise, as compared to gasoline or diesel engine cars. The noise level difference between an electric vehicle and one with an Internal Combustion Engine (ICE) can be as large as 6 dB(A) at 10 km/h, but this

difference becomes smaller at higher speeds. Above approximately 40 km/h, both types of cars are equally loud, because tire noise becomes the most important noise source. In an urban environment, the low sound level emitted at low speeds masked by ambient and traffic noise, makes it more difficult for pedestrians – and much more dramatically for visually impaired ones – to detect an approaching electric vehicle. This was demonstrated by Garay-Vega et al. [1] in a laboratory experiment. Forty-eight visually-impaired participants were surveyed with binaural recordings of conventional or electric vehicles approaching at low speeds (6 mph), in two kinds of background noise, differing in level (31 or 50 dB(A)). They had to detect the approaching car and made their response by pressing a computer key. Results indicated a higher number of missed detections for the electrically driven cars. Also, subjects detected ICE vehicles sooner than the EVs: the difference amounting to as much as 1.5 seconds. At 10 km/h, ICE vehicles were detected at a safe distance (more than 10 m away). In contrast, the electric vehicle was detected only a few meters from the pedestrian, and this can be quite dangerous for a pedestrian intending to cross a road. Indeed, several studies are found in the literature regarding the problem of vehicle detection by visually impaired persons, such as in the work of Verheijen et al [2], Goodes et al [3] or Mendonça et al [4].

In order to prevent this increased risk, manufacturers use, or plan to use, additional warning sounds, emitted by a loudspeaker attached to the front bumper or the wheel arch. Some specifications for these warning sounds already exist. As an example, the U. S. National Highway Traffic Safety Administration recommends values for the frequency bandwidth and sound level of such signals and a similar regulation is currently being prepared by the European authorities. This last project defines acceptable warning sounds in a surprisingly vague manner: they should sound “similar to the sound of a vehicle of the same category equipped with an internal combustion engine and the sound level may not exceed the sound level of a similar internal combustion engine vehicle”. The loudspeakers should deliver a broadband acoustic image, which enables pedestrians to localize the car by the sounds produced. The main frequencies of the warning sounds should be within 200-1000 Hz and no sound should be emitted below 100 Hz. The optimal sound system for electric and hybrid vehicles include three to four speakers- one in each corner of the car- but in principle, two loudspeakers would be sufficient as long as one directs sound forward and one backwards. To obtain the best directional characteristics the loudspeakers should not be hidden in cavities inside the car body but should be able to radiate freely in the wanted directions. However, particular patterns of sound propagation may be observed in urban environments, for example when nearby reflecting surfaces exist, further contributing to the formation of a complex sound field.

This background information clearly indicates the necessity of performing in-depth research regarding the use of standardized AVAS in electric and hybrid vehicles. In this paper, a contribution for discussion of this behaviour is given, in the form of a numerical simulation of the sound field produced by a simple vehicle, under different scenarios. In terms of the urban environment, both an open street and a street with a lateral rigid wall are considered. Regarding the vehicle, two scenarios are considered in terms of loudspeaker distribution, with one or two front-placed speakers. Complementarily, the effect of an obstacle (parked vehicle) is also analyzed, introducing further complexity in the sound propagation patterns. The selected numerical method is the Boundary Element Method, which is particularly well suited for acoustic problems, in which usually an extensive propagation medium exists around the radiating sources. However, standard BEM formulations can pose significant limitations regarding problem size, and special strategies must be used whenever larger problems need to be analyzed. In the present work, an Adaptive-Cross-Approximation algorithm is used, as described in [5], and previously applied by the authors in [6].

THEORETICAL FORMULATION

Governing equations

The propagation of sound within a three-dimensional space can be mathematically represented in the frequency domain by the Helmholtz partial differential equation as:

$$\nabla^2 p + k^2 p = -\sum_{k=1}^{NS} Q_k \delta(\xi_k^f, \xi) \quad (1)$$

where $\nabla^2 = \partial^2/\partial x^2 + \partial^2/\partial y^2 + \partial^2/\partial z^2$, p is the acoustic pressure, $k = \omega/c$, $\omega = 2\pi f$, f is the frequency, c is the sound propagation velocity within the acoustic medium, NS is the number of sources in the domain, Q_k is the magnitude of the existing sources ξ_k^f located at $(x_{\xi_k^f}, y_{\xi_k^f}, z_{\xi_k^f})$, ξ is a domain point located at (x_ξ, y_ξ, z_ξ) and $\delta(\xi_k^f, \xi)$ is the Dirac delta generalized function.

In the above defined Helmholtz equation, the Sommerfeld radiation condition $\lim_{x \rightarrow 0} [\partial p(X)/\partial n - ikp(X)] = 0$ is automatically satisfied at infinity, where X is the field point located at (x, y, z) , n is the unit outward normal vector and $i = \sqrt{-1}$.

Considering that a point source is placed within this propagation domain, at $X_0 = (x_0, y_0, z_0)$, it is possible to establish the fundamental solution for the sound pressure at a point X , at a distance $r = \sqrt{(x-x_0)^2 + (y-y_0)^2 + (z-z_0)^2}$, which can be written as:

$$G(\xi, X) = \frac{e^{-ikr}}{4\pi r} \quad (2)$$

Definition of Green's function using image-sources

In an acoustic analysis, the presence of perfectly reflecting plane surfaces can be taken into account by using the well-known image-source method. In this technique, the effect of a point source in the presence of a given plane surface can be simulated by considering an additional virtual source, positioned in a symmetrical position with respect to the reflecting plane. Thus, following, for example, [6] if such plane is defined by $z=0$, the corresponding Green's function can be written as:

$$G_{half}(\xi, X) = \frac{e^{-ikr}}{4\pi r} + \frac{e^{-ikr_1}}{4\pi r_1} \quad (3)$$

where $r_1 = \sqrt{(x-x_0)^2 + (y-y_0)^2 + (z+z_0)^2}$. The above expression is only valid if the plane is perfectly rigid, with a reflection coefficient of 1.

Boundary Element Method formulation

According to Green's Second Identity, Eq. 0 can be transformed into the following Classic Boundary Integral Equation (CBIE):

$$C(\xi)p(\xi) = -i\rho\omega \int_{\Gamma} G(\xi, X)v_n(X)d\Gamma - \int_{\Gamma} \frac{G(\xi, X)}{\partial n} p(X)d\Gamma + \sum_{k=1}^{NS} Q_k G(\xi_k^f, \xi) \quad (4)$$

where Γ is the boundary surface, ρ is the medium density, $G(\xi_k^f, \xi)$ is the incident field regarding the acoustic pressure generated by the real source placed at position ξ_k^f ; $p(X)$ and $v_n(X)$ represent the acoustic pressure and the normal component of the particle velocity at X , respectively. The coefficient $C(\xi)$ depends on the boundary geometry at the source point, and equals 0.5 for a smooth boundary.

For the case of exterior problems, it is known that equation (4) provides unstable solutions at certain frequencies. Strategies have thus been developed in order to avoid this significant drawback, namely by means of its combination with the so-called Hypersingular Boundary Integral Equation (HBIE). To obtain this second equation, the first derivative with respect to the normal direction at the source point, n_L , must be considered, and the following equation arises:

$$\begin{aligned}
-i\rho\omega\tilde{C}(\xi)v_n(\xi) = & -i\rho\omega\int_{\Gamma}\frac{\partial G(\xi,X)}{\partial n_L}v_n(X)d\Gamma - \\
& \int_{\Gamma}\frac{\partial G(\xi,X)}{\partial n_L\partial n}p(X)d\Gamma + \sum_{k=1}^{NS}Q_k\frac{\partial G(\xi_k^f,\xi)}{\partial n_L}
\end{aligned} \tag{5}$$

As before, the coefficient $\tilde{C}(\xi)$ depends on the boundary geometry at the source point, and equals 0.5 for a smooth boundary.

It has been proposed by Burton and Miller [Erro! Marcador não definido.] that combining the two equations (4) and (5) in the form

$$CBIE + i/k HBIE = 0 \tag{6}$$

originates a new boundary integral equation which provides unique solutions at all frequencies. Different boundary conditions may be prescribed at each boundary element, such as Dirichlet ($p(X) = \bar{p}(X)$), Neumann ($v(X) = \bar{v}(X)$) or Robin ($p(X)/v(X) = \bar{Z}(X)$, being $\bar{Z}(X)$ the acoustic impedance) boundary conditions. After prescribing such conditions, discretizing the boundary into NE_B segments, and establishing adequate interpolation functions within each segment (constant interpolation in the present work), a system with NE_B equations on NE_B unknowns can be assembled. Its solution makes it possible to obtain the acoustic pressure and the normal velocity at each boundary element, and consequently the pressure at any point of the domain can be computed by applying the boundary integral Eq. (4).

Adaptive Cross Approximation formulation

The Adaptive Cross Approximation (ACA) is based in hierarchical matrices (H matrices), an approach that allows for matrix operations with almost linear complexity. These matrices may be understood as an algebraic structure reflecting a geometrically motivated partitioning into sub-blocks, that in turn are classified to be either admissible or not. This block structure points out the fact that the H-matrix arithmetic is easily parallelizable. After having concluded the setup of each block, admissible blocks have to be approximated. The main advantage of ACA is that, for such approximation, it only requires the evaluation of some original matrix entries and the approximation is still almost optimal. Having a matrix $A \in C^{t \times s}$, the approximation is obtained as follow:

$$A \approx S_k = UV^T \tag{6}$$

where $U \in C^{t \times k}$ and $V \in C^{s \times k}$. In this approximation k has a smaller rank when compared with t and s . This low-rank approximation can be obtained only for well-separated computational domains $x \neq y$.

To exploit the full advantages of such approach, it becomes necessary to solve the corresponding equation system by means of an iterative solver. In the present work, the Generalized Minimal Residual Method (GMRES) iterative solver has been used, together with a block preconditioner (to accelerate convergence) based on the non-admissible blocks of the matrix.

NUMERICAL RESULTS

In a first set of examples, let us consider a simple vehicle emitting a warning sound from a single frontal loudspeaker in an open street. The adopted vehicle geometry is only illustrative, and is depicted in Figure 1a. The assemblage of the BEM system matrix is performed as described in the previous section, considering an ACA algorithm, in which admissible blocks are greatly compressed. Figure 1b illustrates the hierarchical matrix constructed for this purpose, where white patches correspond to admissible blocks (composing the vast majority of the matrix). Comparing BEM and ACA-BEM memory requirements, it can be stated that in ACA-BEM the required memory is reduced to 35%.

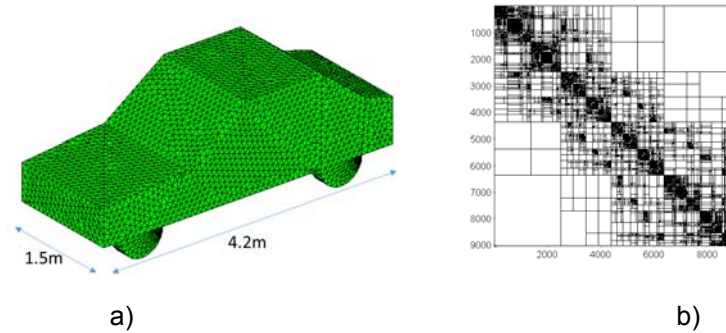


Figure 1: Discretized vehicle using 9056 triangular boundary elements (a) and corresponding ACA-BEM hierarchical matrix representation (b).

For this geometry, sound pressure levels have been calculated considering the single loudspeaker to be placed in the front part, centered with the vehicle. In Figure 2, the sound pressure level in a plane parallel to the ground is illustrated for 250Hz, 500Hz, 750Hz and 1000Hz. It is clear that the increasing excitation frequency originates more intricate SPL maps, with the interaction between direct sound waves and the various reflections being responsible for this complexity. In addition, regions with very low SPL are visible at varying distances, which are generated by the interference between the direct waves and the first reflection on the rigid ground.

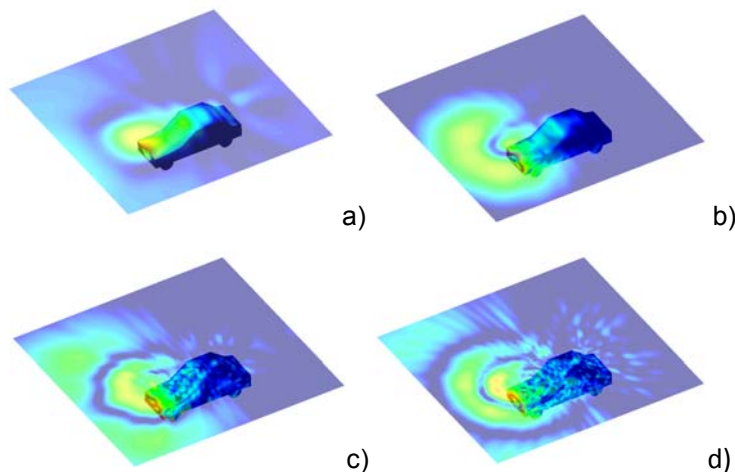


Figure 2: Results for 250Hz (a), 500Hz (b), 750Hz (c) and 1000 Hz (d). Color scale from 15 dB (dark blue) to 75 dB (dark red).

To have a better and clearer view of the observed behavior, polar plots are depicted in Figure 3, considering a distance from the front of the vehicle of 10 m, and for receivers placed 1.6 m above the ground. As stated in the introduction, the distance of 10 m can be considered as the minimum safe distance for vehicle detection by pedestrians, and thus is worth a more detailed analysis.

The polar plots in Figure 3 evidence a distinct directivity pattern, varying with the excitation frequency. For lower frequencies, in spite of the presence of the rigid vehicle shadowing the source, relatively high SPL is reached for all angles, although with somewhat higher values in the front part (a difference of 5 to 10 dB). For the higher frequencies, and as in Figure 2, a more complex behaviour is observed. It is interesting to note for the frequency of 750 Hz a very significant distinction between the front and rear parts of the vehicle, with energy being more concentrated in the front part, as expected.

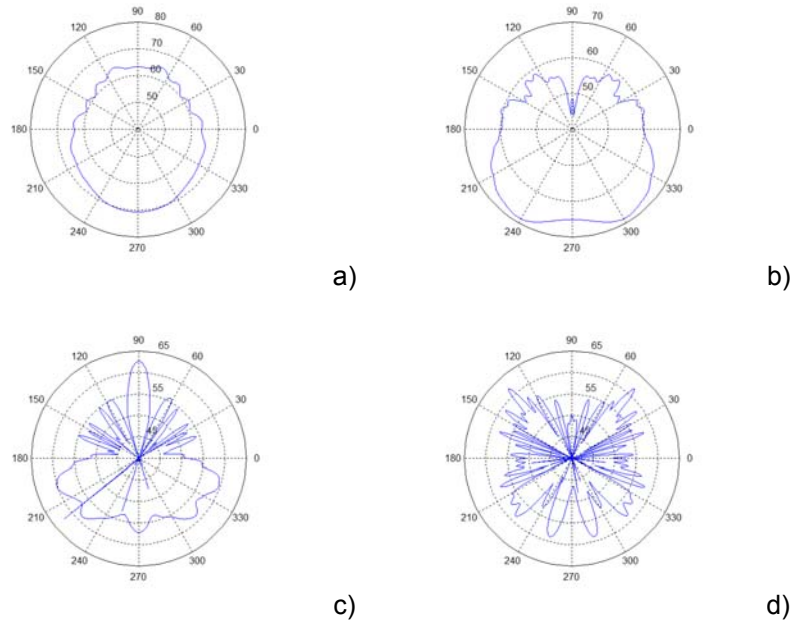


Figure 3: Polar plots for 250Hz (a), 500Hz (b), 750Hz (c) and 1000 Hz (d).

It is important to note that, in the previous simulations, the emitting source was assumed to be a point source placed near the front panel of the vehicle, approximately 0.1 m away from it. Since this is not an exact representation of the real scenario, a second set of simulations was performed embedding this source within the frontal panel, introducing a small semi-spherical cavity where the source is located. A detailed view of the corresponding BEM mesh is depicted in Figure 4a, and the computed polar plots, indicating the directivity of the system, are illustrated in Figure 4b, for a frequency of 750Hz. Comparing with the plots of Figure 3, some differences are visible, in particular in the rear part of the vehicle, where less energy seems to be arriving; by contrast, in the front part, an increase in the SPL is visible, and was to be expected due to the more intense shadowing/baffle effect originated by the cavity where the source is now placed. Remarkably, the main features of the directivity plot in the frontal part are almost exactly maintained, indicating that, for the purpose of evaluating the effect of the source in the front region, using the simpler approach of Figure 1 can be sufficient.

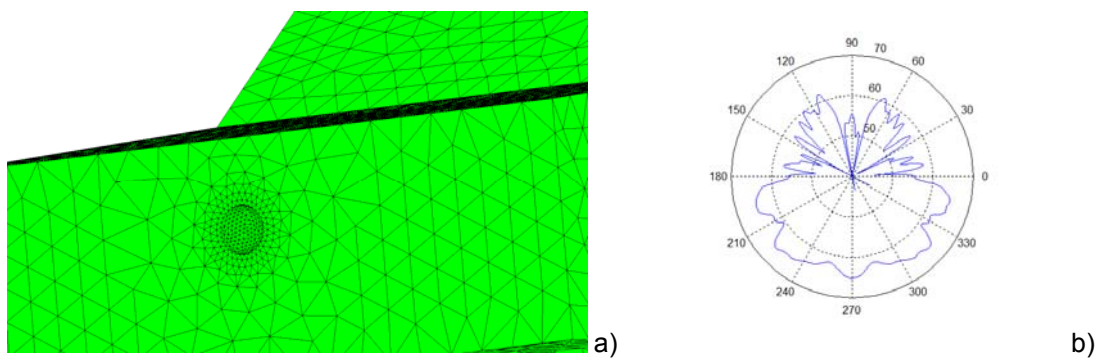


Figure 4: Effect of considering the source embedded in the front panel: (a) detailed view of the BEM mesh and (b) polar plot for a frequency of 750 Hz.

In the previous examples, a single emitting speaker was considered in the front of the vehicle. However, it has been proposed by different researchers that better detectability may be obtained if more sources are placed emitting the warning sound. In the plot of Figure 5, the directivity pattern is compared in polar plots for situations with one and two acoustic sources emitting noise in the frontal part of the vehicle. As expected, the polar plot for the latter case indicates a more dense concentration of energy in front and to both sides of the vehicle; indeed, it is interesting to note that the directivity plot exhibits two broad lobes, one to each side of the

vehicle, where significant and homogenous SPLs are attained, indicating that a significant area is illuminated by the emitting system.

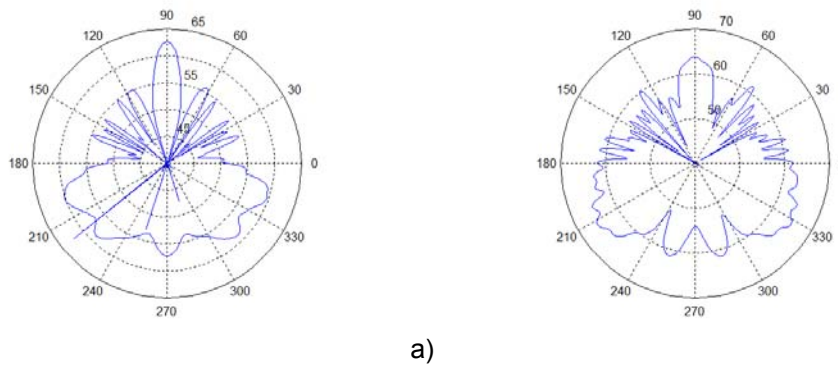


Figure 5: Effect of one (a) or two (b) emitting sources in the front part of the EV, for 750Hz.

In what follows, two distinct situations, usually occurring in an urban environment, are considered, namely the presence of a parked car (obstacle) and the presence of a rigid wall parallel to the street.

Let us start by analyzing the effect of a right-sided parked vehicle, acting as a barrier to the propagation of the warning sounds emitted by the AVAS. Figure 6 illustrates both the SPL and the directivity polar plot for such situation. The SPL color map of Figure 6a clearly indicates the existence of a shadow effect behind the parked vehicle, which, in practice, acts as a barrier to the propagation of sound waves. Observing the polar plot in Figure 6b, this effect is clearly seen, with a significant decrease of the energy reaching the region where pedestrians circulate. Although this decrease is largely dependent on the relative position of the two vehicles, the presented result gives a clear indication regarding a potential acoustic shadowing effect that may decrease detectability of the EVs.

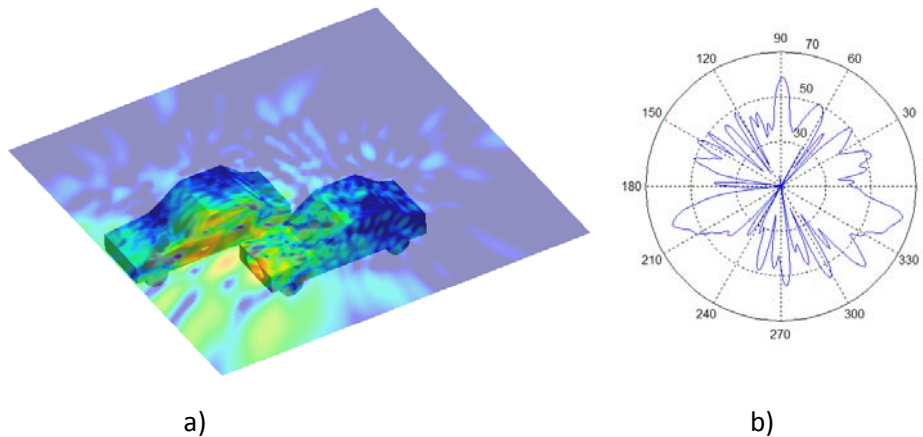


Figure 6: SPL distribution (a) and polar plot (b) calculated in the presence of a parked car, for a frequency of 750Hz.

Results in Figure 7 refer to the last analyzed case, in which a rigid lateral wall is considered parallel to the street. Results for 750Hz and 1000Hz are illustrated. The results, presented in terms of SPL maps, indicate the presence of a reflected field coming from the rigid vertical wall. This reflection enriches the sound field and may slightly increase the detectability of the vehicles by pedestrians. However, it must be stressed that this second wave is traveling from a direction opposite to the car (from the wall side and not from the street side), and can thus induce some confusion as to where the vehicle is situated (particularly in the case of visually impaired people). This behavior merits a more in-depth study, and falls beyond the scope of the present paper.

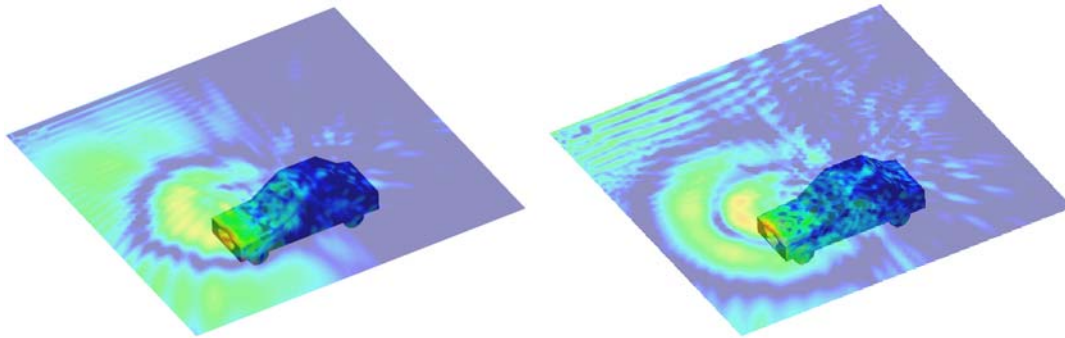


Figure 7: SPL distribution calculated in the presence of a rigid lateral wall, for frequencies of 750Hz (a) and 1000Hz (b).

CONCLUSIONS

This paper presented a numerical approach to the study of the effect of AVAS used in electrical and hybrid vehicles. The “ACA-BEM”, complemented with adequate Green’s functions, is used to conduct the numerical studies considering open and straight-shaped configurations, and in the presence of other vehicles (acting as barriers). Although the objective of the paper is to illustrate the applicability of the numerical tool, it was also possible to draw interesting conclusions regarding the global acoustic behavior of the system. It was observed that the effects of parked vehicles and the urban configuration can greatly influence the capacity of pedestrians to detect circulating vehicles. To finish, it should be noted that further research in this topic is required, and objective quantification of the detectability of these vehicles merits further attention.

ACKNOWLEDGEMENTS

This work was carried out with funding from the General Directorate of Traffic, Spanish Ministry of Interior, through the project whose reference is SPIP2014-01406 (Study and adequacy of warning sounds in electric vehicles).

REFERENCES

- [1] Garay-Vega, L., Hastings, A., Pollard, J. K., Zuschlag, M., & Stearns, M. D. Quieter cars and the safety of blind pedestrians: Phase I (No. HS-811 304), 2010.
- [2] Verheijen, E. Jabben, J. Effect of electric cars on traffic noise and safety. Report 680300009/2010. National Institute for public Health and the Environment Netherlander 2010.
- [3] Goodes, P., Bai Y. B., Meyer, E., Investigation into the Detection of a Quiet Vehicle by the Blind Community and the Application of an External Noise Emitting System. SAE International. 2009-01-21895. 2009.
- [4] Mendonça, C., Freitas, E., Ferreira, J.P., Raimundo, I.D., Santos, J.A. Noise abatement and traffic safety: The trade-off of quieter engines and pavements on vehicle detection. Accident Analysis and Prevention Vol. 51, [11– 17], 2013.
- [5] Liu Y. J., Mukherjee S., Nishimura N., Schanz, M., Ye, W., Sutradhar, A., Pan, E., Dumont, N. A., Fran-gi, A., Saez, A. Recent Advances and Emerging Applications of the Boundary Element Method. Appl. Mech. Rev., 64(3), 030802, 2012.
- [6] Godinho, L., Amado-Mendes, P., Santos, P. G., Cordeiro, M. An efficient and accurate numerical model for the 3d analysis of sonic crystals. 22nd International Congress on Sound and Vibration, Florence, 2015.